EBioMedicine 32 (2018) 201–214

Contents lists available at ScienceDirect

EBioMedicine

journal homepage: www.ebiomedicine.com

Research Paper

Takeda G Protein-Coupled Receptor 5-Mechanistic Target of Rapamycin Complex 1 Signaling Contributes to the Increment of Glucagon-Like Peptide-1 Production after Roux-en-Y Gastric Bypass

Hening Zhai [a,b,1], Zhi Li [a,1], Miao Peng [a,1], Zhaoqi Huang [a], Tingfeng Qin [a], Linxi Chen [a], Hanbing Li [a], Heng Zhang [a], Weizhen Zhang [c,d], Geyang Xu [a,*]

[a] Department of Physiology, School of Medicine, Jinan University, 601 Huangpu Avenue West, Tianhe District, Guangzhou, Guangdong 510632, China
[b] Endoscopy Center, The First Affiliated Hospital of Jinan University, 613 Huangpu Avenue West, Tianhe District, Guangzhou, Guangdong 510630, China
[c] Shenzhen University Diabetes Center, Shenzhen University Health Science Center, Shenzhen, Guangdong 518060, China
[d] Department of Surgery, University of Michigan Medical Center, Ann Arbor, MI 48109-0346, USA

ARTICLE INFO

Article history:
Received 22 December 2017
Received in revised form 20 May 2018
Accepted 21 May 2018
Available online 30 May 2018

Keywords:
Deoxycholic acid
GLP-1
mTORC1
RYGB
TGR5

ABSTRACT

Background: The mechanism by which Roux-en-Y Gastric Bypass (RYGB) increases the secretion of glucagon-like peptide-1 (GLP-1) remains incompletely defined. Here we investigated whether TGR5-mTORC1 signaling mediates the RYGB-induced alteration in GLP-1 production in mice and human beings.
Methods: Circulating bile acids, TGR5-mTORC1 signaling, GLP-1 synthesis and secretion were determined in lean or obese male C57BL/6 mice with or without RYGB operation, as well as in normal glycemic subjects, obese patients with type 2 diabetes before and after RYGB.
Results: Positive relationships were observed among circulating bile acids, ileal mechanistic target of rapamycin complex 1 (mTORC1) signaling and GLP-1 during changes in energy status in the present study. RYGB increased circulating bile acids, ileal Takeda G protein-coupled receptor 5 (TGR5) and mTORC1 signaling activity, as well as GLP-1 production in both mice and human subjects. Inhibition of ileal mTORC1 signaling by rapamycin significantly attenuated the stimulation of bile acid secretion, TGR5 expression and GLP-1 synthesis induced by RYGB in lean and diet-induced obese mice. GLP-1 production and ileal TGR5-mTORC1 signaling were positively correlated with plasma deoxycholic acid (DCA) in mice. Treatment of STC-1 cells with DCA stimulated the production of GLP-1. This effect was associated with a significant enhancement of TGR5-mTORC1 signaling. siRNA knockdown of mTORC1 or TGR5 abolished the enhancement of GLP-1 synthesis induced by DCA. DCA increased interaction between mTOR-regulatory-associated protein of mechanistic target of rapamycin (Raptor) and TGR5 in STC-1 cells.
Interpretation: Deoxycholic acid-TGR5-mTORC1 signaling contributes to the up-regulation of GLP-1 production after RYGB.

1. Introduction

The increase in incidence and prevalence of type 2 diabetes is strongly associated with the obesity epidemic [1]. Roux-en-Y gastric bypass (RYGB) is the most effective approach for weight loss and randomized, controlled trials demonstrate its superiority compared to medical therapy for diabetes control [2,3]. Mechanisms underlying diabetes resolution in RYGB remain unclear, limiting development of less-invasive alternatives. Numerous studies have documented post-RYGB hormonal changes [4–7]. One of the changes known to occur after RYGB is an increase in postprandial glucagon-like peptide-1 (GLP-1) concentrations compared with control subjects [8–10]. GLP-1 is an insulin secretagogue released by enteroendocrine L cells [11]. In addition to its incretin effect, GLP-1 delays gastric emptying, enhances satiation, reduces food intake,

Abbreviations: BAs, Bile acids; Cyp7a1, Cytochrome P450 family 7 subfamily A member 1; DCA, Deoxycholic acid; FXR, Farnesoid X receptor; GLP-1, Glucagon-like peptide-1; ip, Intraperitoneal; mTOR, mechanistic target of rapamycin; mTORC1, mechanistic target of rapamycin complex 1; Raptor, Regulatory-associated protein of mechanistic target of rapamycin; RYGB, Roux-en-Y gastric bypass; S6, Ribosomal protein S6; S6K1, Ribosomal protein subunit 6 kinase 1; TGR5, Takeda G protein-coupled receptor 5.

* Corresponding author at Jinan University, No. 601, West Huangpu Avenue, Tianhe District, Guangzhou, Guangdong, 510632, China. Tel.: 0086 20 85220260; Fax: 0086 20 85221343
E-mail addresses: weizhenz@umich.edu (W. Zhang), xugeyangliang@163.com (G. Xu).
[1] These authors contributed equally to this work.

https://doi.org/10.1016/j.ebiom.2018.05.026

suppresses glucagon secretion, and regulates hepatic and peripheral glucose flux [12,13]. GLP-1 circulates as two active forms, GLP-1 (7–37) and GLP-1 (7–36) amide, and both of them improve glucose homeostasis and control body weight in experimental models of diabetes and obesity [14,15]. These and numerous other observations have led to the development of GLP-1-based therapies for type 2 diabetes [16,17]. Accordingly, an understanding of how RYGB alters GLP-1 production will facilitate the development of less-invasive therapies for weight loss and metabolic control that can be more broadly applied than surgery.

Recent researches illustrate that fasting GLP-1 levels are positively associated with total, secondary and conjugated bile acids after RYGB surgery [18]. Bile acids are signaling molecules that coordinately regulate metabolism and inflammation via their hormone receptors nuclear farnesoid X receptor (FXR) and Takeda G protein-coupled receptor 5 (TGR5) [19]. TGR5 contributes to the glucoregulatory benefits of vertical sleeve gastrectomy (VSG) surgery by promoting metabolically favorable shifts in the circulating bile acid pool [20,21]. Bile acids may also act as molecular enhancers of GLP-1 secretion through activation of TGR5-receptors [22,23]. However, the molecular mechanisms by which intestinal L cells sense the change of circulating bile acids at the organism level to regulate GLP-1 production after RYGB are currently unknown.

Mechanistic target of rapamycin (mTOR), a highly conserved serine-threonine kinase, has been reported to serve as an intracellular fuel sensor critical for energy homeostasis [24,25]. Aberrant mTOR activity is linked to the development of cancer, diabetes, and obesity [26]. Downstream targets of mTOR include ribosomal protein S6 kinases (S6Ks), S6 and eukaryotic translation initiation factor 4E binding protein 1 (4EBP1) [26,27]. Deletion of S6K1 protects against while 4EBP1 gene null worsens glucose metabolism in diet-induced obese mice [28,29] There are two mTOR complexes: mTOR complex 1 (mTORC1) and mTOR complex 2 (mTORC2). mTORC1 is responsible for nutrient-sensing functions and is composed of mTOR, G protein-subunit-like protein, and regulatory-associated protein of mechanistic target of rapamycin (Raptor). mTORC2 which phosphorylates Akt contains mTOR and rapamycin-insensitive companion of mTOR (Rictor) [25] Our previous studies demonstrate that ileal mTORC1 signaling regulates the production of GLP-1 [30]. We thus hypothesized that mTORC1 is required for the effects of RYGB on GLP-1 production. Here, we examined whether bile acids-induced TGR5-mTORC1 signaling pathway contributes to the increment of GLP-1 production after RYGB in the mouse obese models and human subjects.

2. Material and Methods

2.1. Animals and Treatments

Male C57BL/6J mice were maintained at a regulated environment (24 °C, 12-h light, 12-h dark cycle with lights on at 0700 and off at 1900). Regular chow (NCD: 3.85 kcal/g, 10% fat, 20% protein, 70% carbohydrate, formula D12450B, Research Diets Inc., New Brunswick, NJ, USA) or high-fat diet (5.24 kcal/g, 60% fat, 20% protein, 20% carbohydrate, formula D12492, Research Diets Inc.) was available ad libitum unless specified otherwise. Animals used in this study were handled in accordance with the Guide for the Care and Use of Laboratory Animals published by the US National Institutes of Health (NIH Publication No. 8023, revised 1978). All animal protocols were approved by the Laboratory Animal Ethics Committee of Jinan University.

When indicated, animals were fasted for 24 h, treated with dimethyl sulfoxide (DMSO) or rapamycin (1 mg/kg) for 9 consecutive days, or injected via tail veins with adenovirus containing green fluorescent protein (Ad-GFP, 10^9 pfu) or adenovirus containing ribosomal protein subunit 6 kinase 1 (Ad-S6K1, 10^9 pfu) 9 days before sacrifice.

2.2. Surgical Procedures

RYGB and sham surgeries were performed as previously described [31,32]. Animals were fasted 4 to 6 h before the operation. Anesthesia was induced and maintained with isoflurane. Standard aseptic procedures were used throughout.

RYGB surgery: A small gastric pouch with a volume of approximately 5% of the normal gastric volume was anastomosed with the open end of the jejunum. The jejunum was transected about 6 cm distal to the pylorus. The distal end was brought up to the stomach pouch for an end to end anastomosis. For the jejuno-jejunostomy, a longitudinal slit was made on the antimesenteric side of the jejunum at 6 cm distal to the site of gastrojejunostomy, and the proximal end of the jejunum was joined in an end-to-side anastomosis. Before the closing of the abdominal cavity, the intestine was arranged in an “S” position to avoid intestinal obstruction. In the abdominal wall, the muscular and skin layers were closed separately.

Sham operation: the perigastric ligaments were cut, and then a 3 mm incision was made in the stomach wall and closed with a titanium clip. In addition, the jejunum was transected 6 cm distal to the pylorus, and the two cut ends were anastomosed.

Post-operative care: Mice were given 0.7 mL of 5% dextrose subcutaneously and carprofen (5 mg/kg, s.sc) for analgesia after surgery. Mice were allowed to recover under previously described post-operative care [33]. A liquid diet was provided on post-surgery days 2 through 5. On post-operative days 6 and 7, 0.25 g high-fat diet was provided and on post-surgery day 8, a high-fat diet or normal chow diet was provided ad libitum.

2.3. Recruitment of Human Subjects and Collection of Intestinal Biopsies

Six male obese participants with type 2 diabetes, six one-year post-RYGB patients and six normal glycemic subjects were enrolled in the study. Anthropometric data are provided in Supplementary Table 1. Participation in this study was voluntary and written informed consent was obtained from each participant. The guidelines of the Declaration of Helsinki of the World Medical Association were followed. All protocols were approved by the Research Ethics Committee of the First Affiliated Hospital of Jinan University. All participants were fasted for 12 h. An enteroscopy was performed in sedated participants using a colonoscopy (CF-HQ290I; Olympus). Mucosal biopsies were taken from intestines. Tissue samples were extracted for protein and RNA or for immunohistochemistry, respectively.

2.4. Cell Culture, Transfection and Reporter Assays

STC-1 cells were maintained in DMEM medium supplemented with 2.5% fetal bovine serum and 10% horse serum at 37 °C in an atmosphere of 5% CO_2 air [34].

For transient transfection, cells were plated at optimal densities and grown for 24 h. Cells were then transfected with TGR5 siRNA or mTOR siRNA using lipofectamine reagent according to the manufacturer's instructions. After 24 h transfection, the cells were then treated with DMSO or DCA (30 μmol/L) for another 24 h.

For reporter assays, cells were plated onto 24-well tissue culture plates at optimal densities and grown for 24 h. Cells were then transfected with the proglucagon promoter-luciferase reporter gene constructs (500 ng) and an internal control pSV-β-galactosidase (25 ng) per well using lipofectamine reagent [30]. Cells were treated with various doses of deoxycholic acid (DCA) for 24 h. Cell lysates were analyzed for luciferase activity with the luciferase reporter assay system using a luminometer (Monolight 2010, Analytical Luminescence Laboratory, SanDiego, CA) according to the manufacturer's instructions. β-galactosidase activity was measured according to the manufacturer's protocol.

2.5. Co-immunoprecipitation (Co-IP)

For co-immunoprecipitation, STC-1 cells treated with DCA (30 μmol/L) or DMSO for 24 h were lysed with RIPA lysis buffer for 30 min and

centrifuged at 12,000*g* for 15 min. Total proteins (500 μg) were incubated with indicating primary antibodies such as TGR5, mTOR or Raptor. The mixture was gently rotated at 4 °C overnight. Anti-rabbit IgG antibody was served as negative control. The immunocomplex was collected with protein A+G agarose, and the precipitates were washed five times with ice-cold PBS. Finally, proteins were released by boiling in sample buffer and utilized for western blot analysis.

2.6. Analysis of Circulating Bile Acids

To determine the concentration of BAs in plasma, BAs were measured with a highly selective reversed phase LC-MS/MS analysis method in negative MRM detection mode. Data of BAs were processed with Analyst Software 1.5, ACD/Labs ChemSketch and EXCEL 2010 software for comprehensive statistical analysis. BA panel comprised cholic acid (CA), chenodeoxycholic acid (CDCA), deoxycholic acid (DCA), 3β-cholic acid (3β-CA), ursodeoxycholic acid (UDCA), hyodeoxycholic acid (HDCA), isodeoxycholic acid (IDCA), 23-norcholic acid (NCA), ursocholic acid (UCA), 3-dehydrocholic acid (3-DHCA), 7-ketodeoxycholic acid (7-KDCA), 7-ketolithocholic acid (7-KLCA), allocholic acid (ALCA), α-, β- and λ-muricholic acid (MCA) as well as their glycine (G) and taurine (T) conjugates. Taurodehydrocholic acid, tauro-β-muricholic acid, tauro-ω-muricholic acid, dehydrolithocholic acid, isolithocholic acid, 23-nordeoxycholic acid, 6-ketolithocholic acid, 12-ketolithocholic acid, apocholic acid, 3β-ursodeoxycholic acid, β-hyodeoxycholic acid, dehydrocholic acid, dioxolithocholic acid, 6,7-diketolithocholic acid and 12-dehydrocholic acid were excluded from calculations due to undetectable plasma concentrations. For calculations, BAs were further grouped as follows: 1) total BAs = all BAs including conjugated and free forms; 2) primary BAs = CA, CDCA, 3β-CA, NCA, UCA, α-, β-MCA and conjugates; 3) secondary BAs = DCA, UDCA, IDCA, ALCA, HDCA, 7-KLCA, 7-KDCA, 3-DHCA, λ-MCA and their conjugates; 4) unconjugated BAs = CA, CDCA, DCA, 3β-CA, NCA, UCA, 3-DHCA, 7-KDCA, 7-KLCA, ALCA, HDCA, IDCA, UDCA, α-, β- and λ-MCA; 5) conjugated BAs = all glycine- and taurine-conjugated BAs.

2.7. Western Blot Analysis

Protein extracts were electrophoresed, blotted, and then incubated with primary antibodies. The antibodies were detected using 1:10,000 horseradish peroxidase-conjugated, donkey anti-rabbit IgG and donkey anti-mouse IgG (Jackson ImmunoResearch, USA). A western blotting luminol reagent was used to visualize bands corresponding to each antibody. The band intensities were quantitated by Image J software.

2.8. Immunohistochemistry

Intestinal mucosal biopsies were postfixed in 4% paraformaldehyde, dehydrated, embedded in wax, and sectioned at 6 μm. Paraffin-embedded sections were dewaxed, rehydrated and rinsed in PBS. After boiling for 10 min in 0.01 mol/L sodium citrate buffer (pH 6.0), sections were blocked in 5% goat preimmune serum in PBS for 1 h at room temperature and then incubated overnight with rabbit anti-Phospho-S6K (Thr389) (1:100), Phospho-S6 (Ser235/236) (1:400) or rabbit anti-TGR5 (1:500) combined with mouse monoclonal antibody to GLP-1 (1:500). Tissue sections were then incubated at 22 °C for 2 h with a mixture of the following secondary antibodies: goat anti-mouse fluorescein isothiocyanate-conjugated IgG (1:50) and dylight 594 affinipure donkey anti-rabbit IgG (1:100). Controls included substituting primary antibodies with mouse IgG or rabbit IgG. Photomicrographs were taken under a confocal laser-scanning microscope (Leica, Germany).

2.9. Quantitative Real-Time PCR

Quantitative Real-time PCR was performed as described previously [30,34]. Primers used in this study were shown in Supplementary Table 2. For gene expression analysis, RNA was isolated from mouse tissues using TRIzol and reverse-transcribed into cDNAs using the First-Strand Synthesis System for RT-PCR kit. SYBR Green-based real-time PCR was performed using the Mx3000 multiplex quantitative PCR system (Stratagene, La Jolla, CA). Triplicate samples were collected for each experimental condition to determine relative expression levels.

2.10. Measurements of GLP-1

Measurements of GLP-1 secretion were performed as described previously [30,34] Samples were collected in the presence of aprotinin (2 μg/mL), EDTA (1 mg/mL) and diprotin A (0.1 mmol/L), and stored at −80 °C before use. Total and active forms of GLP-1 were assayed using the enzyme immunoassay kits according to the manufacturer's instructions.

2.11. Statistical Analysis

Statistical differences were evaluated by factorial design analysis of variance (ANOVA) or one-way ANOVA followed by Newman-Student-Keuls test. Comparisons between two groups were performed using Student's t-test. The correlation was determined by Pearson analysis. $P < 0.05$ was considered significant.

3. Results

3.1. Effects of Fasting on Plasma TBAs, Intestinal mTORC1 Signaling, and GLP-1 Production

To examine the effect of organism energy status on plasma total bile acids, mTORC1 signaling and GLP-1 production in different intestinal segments, 12-week-old male C57BL/6 J mice were divided into two groups, a control group in which animals were fed ad libitum and a group in which mice were fasted for 24 h. Fasting significantly reduced plasma TBAs (Supplementary Fig. 1c). Alteration in plasma bile acids was associated with significant decreases in the phosphorylation of S6 ribosomal protein and GLP-1 precursor named proglucagon in jejunum and ileum but not in duodenum in fasted mice. Both S6 activity and proglucagon expression of jejunum and ileum were higher than duodenum in fed mice (Supplementary Fig. 1a). In addition, proglucagon mRNA levels were significantly decreased in fasted intestines relative to controls (Supplementary Fig. 1b). Correlation between plasma TBAs, ileal levels of phospho-S6 and proglucagon expressions was significantly positive (Supplementary Fig. 1d).

3.2. Attenuation of RYGB's Effects on Circulating Bile Acids, Ileal TGR5-mTORC1 Signaling and GLP-1 Production by Rapamycin in C57BL/6J Mice

RYGB stimulates GLP-1 synthesis and secretion [10,35] Our previous studies show that mTORC1 is an intestinal fuel sensor whose activity is linked to the regulation of GLP-1 [30]. We thus hypothesized that RYGB enhanced GLP-1 production through mTORC1 signaling. The effects of rapamycin, a well-documented mTORC1 inhibitor, were first examined. Obese mice induced by 60% high fat diet for 16 weeks were randomly divided into four groups: sham group receiving dimethyl sulfoxide (DMSO), sham group receiving rapamycin (1 mg/kg) ip injection for 9 days, RYGB-operated mice receiving DMSO or rapamycin. RYGB significantly stimulated the mTORC1 signaling in ileal mucosa as evidenced by the increase in raptor, as well as the phosphorylation levels of mTOR and its downstream targets: S6K1 and S6 (Fig. 1a). The increase in the mRNA and protein levels of ileal TGR5 and Cyp7a1, a rate-limited enzyme in the biosynthesis of bile acids [36], was associated with the activation of ileal mTORC1 signaling (Fig. 1a, b, and e). Surprisingly, RYGB suppressed the expression of FXR and its downstream effector small heterodimer partner (SHP) in ileums (Fig. 1a, c, and d). Consistent with previous reports, ileal proglucagon mRNA, protein and plasma

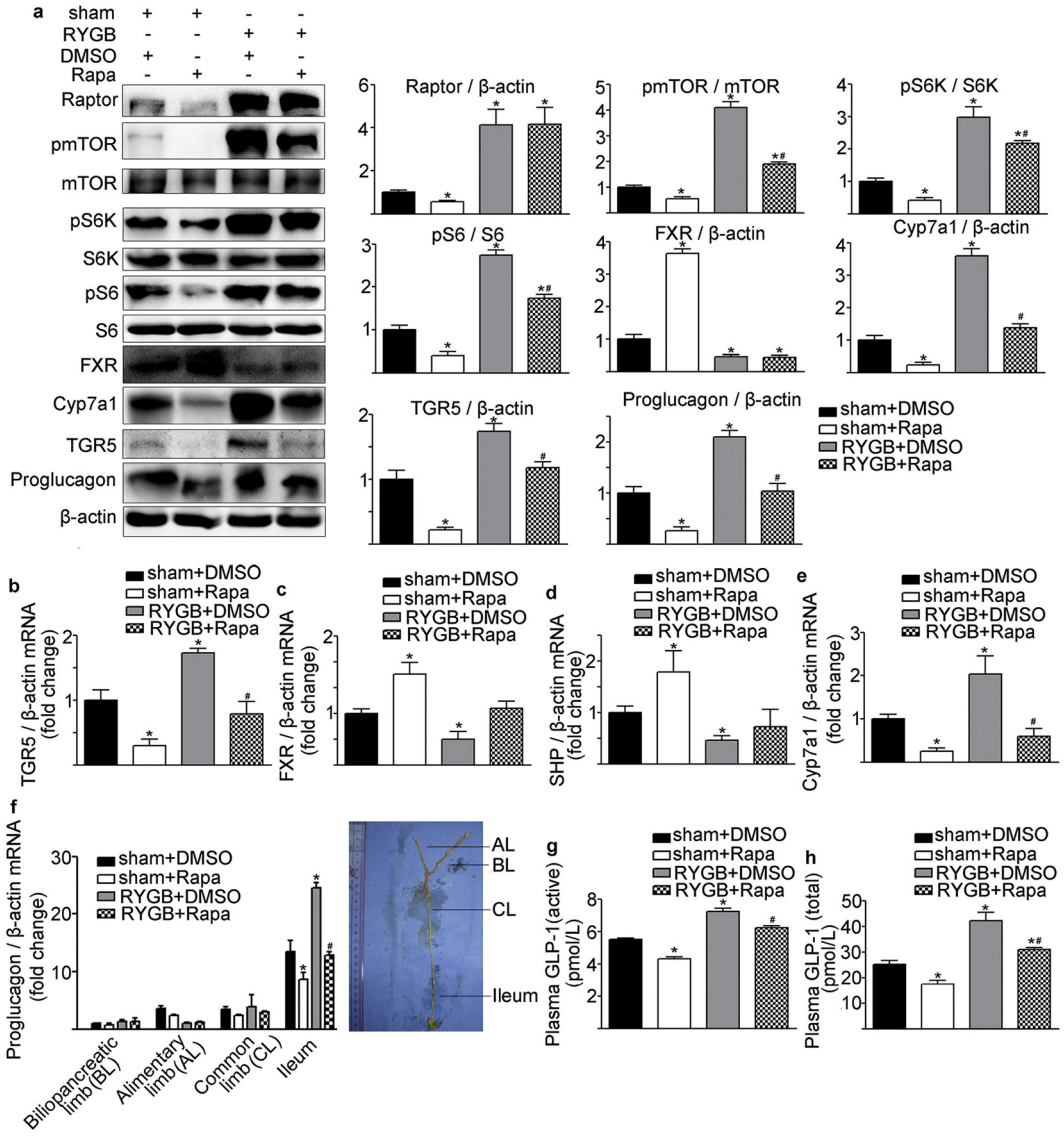

Fig. 1. Effects of rapamycin on RYGB-induced alteration of ileal TGR5-mTORC1 signaling and GLP-1 production in DIO mice. (a) Representative western blots from sham- or RYGB-operated mice that received ip injection of DMSO, rapamycin (Rapa, 1 mg/kg). Raptor, pmTOR, mTOR, pS6K, S6K, pS6, S6, FXR, Cyp7a1, TGR5, proglucagon, and β-actin were detected using specific antibodies. Results of quantitative PCR analysis of TGR5 mRNA (b), FXR mRNA (c), SHP mRNA (d), Cyp7a1 mRNA (e) in mouse ileums and proglucagon mRNA in different intestinal segments (f) are expressed as fold change from control using β-actin as loading control. (g) Plasma GLP-1(active). (h) Plasma GLP-1(total). Six samples were examined for each condition. *, $P < 0.05$ vs. sham-operated mice receiving DMSO. #, $P < 0.05$ vs. RYGB- operated mice receiving DMSO. Statistical differences were evaluated by factorial design analysis of variance (ANOVA).

GLP-1 were stimulated by RYGB (Fig. 1a, f, g, and h). Interestingly, this phenomenon was only observed in ileums but not in other intestinal segments such as biliopancreatic limbs, alimentary limbs and common limbs (Fig. 1f). Pre-treatment with rapamycin significantly attenuated the alteration of ileal mTORC1 signaling, TGR5, and Cyp7a1 as well as GLP-1 production induced by RYGB (Fig. 1a–h).

In L cells, activation of FXR decreased proglucagon expression [37], whereas bile acids promote GLP-1 secretion through TGR5 [23,38] We thus examined the alteration of circulating bile acid composition in sham- and RYGB-operated DIO mice. A significant increase of total BAs was observed in 6-week post-RYGB mice relative to sham animals (1897.0 ± 223.4 to 8825.0 ± 96.9 nmol/L, $P < 0.01$) (Table 1). Pearson analysis showed that plasma deoxycholic acid, an unconjugated BA, was positively correlative with GLP-1 production and TGR5-mTORC1 signaling in the ileal mucosa of mice with sham or RYGB surgery (Supplementary Table 3). Although rapamycin significantly suppressed plasma total BAs (1897.0 ± 223.4 to 732.4 ± 37.5 nmol/L, $P < 0.01$) in the sham animals, it demonstrated no effect on the up-regulation of total BAs, primary and secondary BAs elicited by RYGB (Table 1). RYGB-induced increase in unconjugated BAs such as DCA, a secondary agonist for both TGR5 and FXR receptors, was significantly reversed by rapamycin. On the other hand, rapamycin further increased the up-regulation of conjugated BAs such as TCA and TUDCA induced by RYGB (Table 1).

Rapamycin also attenuated the RYGB-elicited alteration on ileal TGR5-mTORC1 signaling and GLP-1 production in lean mice (Supplementary Fig. 2).

3.3. Additional Effects of S6K1 Overexpression and RYGB on Ileal TGR5-mTORC1 Signaling, GLP-1 Production and Plasma Bile Acid Composition in DIO Mice

We next examined whether activation of mTORC1 signaling in the ileums would enhance the effect of RYGB on the production of GLP-1. Tail vein administration of Ad-S6K1 (10^9 pfu), a downstream target of mTOR, significantly increased both phospho-S6K and phospho-S6 levels

Table 1
RYGB alters plasma BA composition and concentrations in DIO mice receiving rapamycin or not.

Specific BAs	HSD	HSR	HRD	HRR
3β-CA	33.0 ± 5.9	10.4 ± 2.5*	128.7 ± 4.9†	57.0 ± 1.9‡,§
CA	135.7 ± 30.1	66.9 ± 8.0	530.3 ± 19.6†	361.4 ± 10.6‡,§
CDCA	27.6 ± 5.9	19.8 ± 3.3	31.6 ± 4.8	34.2 ± 4.3
NCA	11.6 ± 1.7	7.3 ± 1.0	16.7 ± 2.4	10.0 ± 0.1§
UCA	9.2 ± 2.7	4.4 ± 0.4	25.3 ± 8.7	9.3 ± 1.5§
α-MCA	17.7 ± 3.3	5.8 ± 0.7*	64.4 ± 2.1†	62.8 ± 17.3
β-MCA	126.5 ± 18.4	23.1 ± 2.5*	1206.0 ± 205.6†	325.9 ± 15.9‡,§
3-DHCA	10.6 ± 1.4	3.9 ± 0.7*	27.5 ± 3.6†	26.3 ± 3.8‡
7-KDCA	25.7 ± 3.6	19.5 ± 2.0	74.2 ± 0.9†	44.3 ± 5.9§
7-KLCA	23.9 ± 10.5	25.5 ± 8.1	21.7 ± 4.3	14.1 ± 0.7
ALCA	17.5 ± 0.5	7.1 ± 1.7*	62.2 ± 1.2†	33.9 ± 0.9‡,§
DCA	111.7 ± 10.5	68.2 ± 1.9*	528.1 ± 5.1†	223.6 ± 10.8‡,§
HDCA	19.3 ± 7.9	23.8 ± 9.9	25.0 ± 0.4	64.4 ± 39.3
IDCA	7.6 ± 1.6	5.9 ± 1.2	11.5 ± 1.2	10.4 ± 4.4
UDCA	14.5 ± 2.4	8.8 ± 1.7	75.0 ± 14.9†	39.2 ± 3.2‡,§
λ-MCA	18.1 ± 0.1	2.8 ± 1.7*	21.7 ± 0.8†	10.1 ± 2.4‡
GCA	10.7 ± 0.3	3.2 ± 2.2*	17.7 ± 2.4†	14.3 ± 0.7‡,§
GCDCA	12.9 ± 0.8	11.6 ± 0.9	15.0 ± 1.5	12.2 ± 1.7
TCA	373.2 ± 71.9	49.4 ± 6.0*	1666.0 ± 128.1†	2943.0 ± 175.6‡,§
α-TMCA	277.8 ± 14.9	218.4 ± 12.6*	1508.0 ± 413.7†	1641.0 ± 565.8
GDCA	11.0 ± 0.5	9.3 ± 0.4	11.3 ± 0.9	9.8 ± 0.6
GDHCA	6.6 ± 0.8	5.1 ± 0.9	5.6 ± 1.2	5.7 ± 0.4
GHDCA	9.7 ± 0.2	8.8 ± 0.2	10.3 ± 0.7	9.1 ± 0.3
GLCA	10.4 ± 1.5	1.8 ± 0.6*	15.4 ± 2.7	9.2 ± 1.1§
GUDCA	12.0 ± 0.9	11.0 ± 1.0	15.7 ± 1.0†	10.0 ± 0.4§
TDCA	51.0 ± 2.8	26.3 ± 13.1	144.3 ± 33.3†	75.9 ± 3.2‡,§
THDCA	7.8 ± 1.0	1.5 ± 0.8*	9.8 ± 0.5	20.2 ± 5.6§
TLCA	6.4 ± 1.2	6.3 ± 2.7	9.0 ± 2.3	5.1 ± 1.2
TUDCA	36.6 ± 1.6	16.6 ± 1.3*	128.0 ± 12.7†	215.0 ± 46.3‡,§
λ-GMCA	18.4 ± 1.6	15.1 ± 3.4	14.4 ± 0.8	13.8 ± 2.9
λ-TMCA	442.2 ± 145.5	49.8 ± 12.4	2405.0 ± 24.8†	4261.0 ± 791.5‡,§
Total BAs	1897.0 ± 223.4	732.4 ± 37.5*	8825.0 ± 96.9†	10,570.0 ± 1615.0‡
Unconjugated BAs	610.1 ± 51.0	298.3 ± 16.5*	2850.0 ± 202.4†	1327.0 ± 34.0‡,§
Conjugated BAs	1287.0 ± 201.8	434.1 ± 33.4*	5976.0 ± 272.8†	9244.0 ± 1587.0‡,§
Primary BAs	1036.0 ± 96.1	412.7 ± 13.8*	5209.0 ± 100.2†	5470.0 ± 740.3‡
Secondary BAs	861.5 ± 131.4	306.7 ± 30.0*	3616.0 ± 43.3†	5101.0 ± 875.2‡

Values are presented as the mean ± SEM. All bile acids are presented in concentrations of nmol/L (n = 4 per group).
* $P < 0.05$ within sham-operated mice receiving DMSO (HSD) vs sham group receiving rapamycin (HSR).
† $P < 0.05$ within HSD vs RYGB-operated mice receiving DMSO (HRD).
‡ $P < 0.05$ within HSD vs RYGB-operated mice receiving rapamycin (HRR).
§ $P < 0.05$ within HRD vs HRR.

in ileal mucosa (Fig. 2a), suggesting the activation of mTORC1 signaling. Both overexpression of S6K1 and RYGB enhanced the mTORC1 activity. This alteration was followed by a significant increase in mRNA and protein levels of ileal TGR5 and Cyp7a1 (Fig. 2a, b, and e), and the concomitant decrease in ileal FXR and SHP (Fig. 2a, c, and d). Both overexpression of S6K1 and RYGB significantly stimulated GLP-1 synthesis and secretion. Further, RYGB combined with injection of Ad-S6K1 also significantly stimulated GLP-1 production relative to sham-operated mice receiving Ad-GFP (Fig. 2a, f, g, and h).

We also examined the co-localization of TGR5 and GLP-1 in ileal L cells using double-labeling immunofluorescent staining. Antibodies recognizing TGR5 and GLP-1 demonstrated strong positive reactivity in ileums. RYGB significantly increased the signal intensity for TGR5 and GLP-1 relative to sham surgery. Overexpression of S6K1 also enhanced TGR5, GLP-1 staining in sham mice. RYGB combined with administration of Ad-S6K1 also significantly increased TGR5 and GLP-1 staining when compared to sham-operated mice receiving Ad-GFP (Fig. 3).

As shown in Table 2, RYGB significantly increased total BAs, unconjugated and conjugated BAs in either Ad-GFP or Ad-S6K1 treated animals. Again, DCA was significantly increased by RYGB and overexpression of S6K1. Under conditions of RYGB combined with tail vein administration of Ad-S6K1, GLP-1 production and TGR5-mTORC1 signaling were positively correlative with plasma deoxycholic acid (Supplementary Table 4).

3.4. Effects of RYGB on Intestinal TGR5-mTORC1 Signaling and GLP-1 Expression in Human Beings

We further examined the effects of RYGB on intestinal mTORC1 signaling activity and GLP-1 expression in human subjects. As shown in Fig. 4, enhanced mTORC1 signaling activity in ileums as evidenced by an increase in raptor, phosphorylation levels of mTOR, S6K1, and S6 was observed in post-RYGB subjects or non-diabetic subjects when compared to obese type 2 diabetic patients. This change was associated with inhibition of ileal FXR and SHP expression. No difference was detected between post-RYGB and non-diabetic subjects (Fig. 4a, c, and d). mRNA and protein levels of TGR5 and Cyp7a1 in ileal mucosa were markedly down-regulated in obese type 2 diabetics relative to either post-RYGB or non-diabetic subjects (Fig. 4a, b, and e). Both the mRNA and protein levels of proglucagon in ileal mucosa were significantly decreased in obese type 2 diabetic patients versus post-RYGB subjects or non-diabetics. (Fig. 4a and f). There existed a positive relation between ileal mTORC1 activity and proglucagon expression (Fig. 4a). Details of clinical information on human subjects are presented in Supplementary Table 1.

Antibodies recognizing TGR5, phospho-S6K (Thr389), phospho-S6 (Ser235/236) and GLP-1 demonstrated stronger positive reactivity in ileums of post-operative patients compared to obese type 2 diabetic patients (Fig. 5), suggesting that RYGB increases ileal TGR5-mTORC1 signaling and GLP-1 expression.

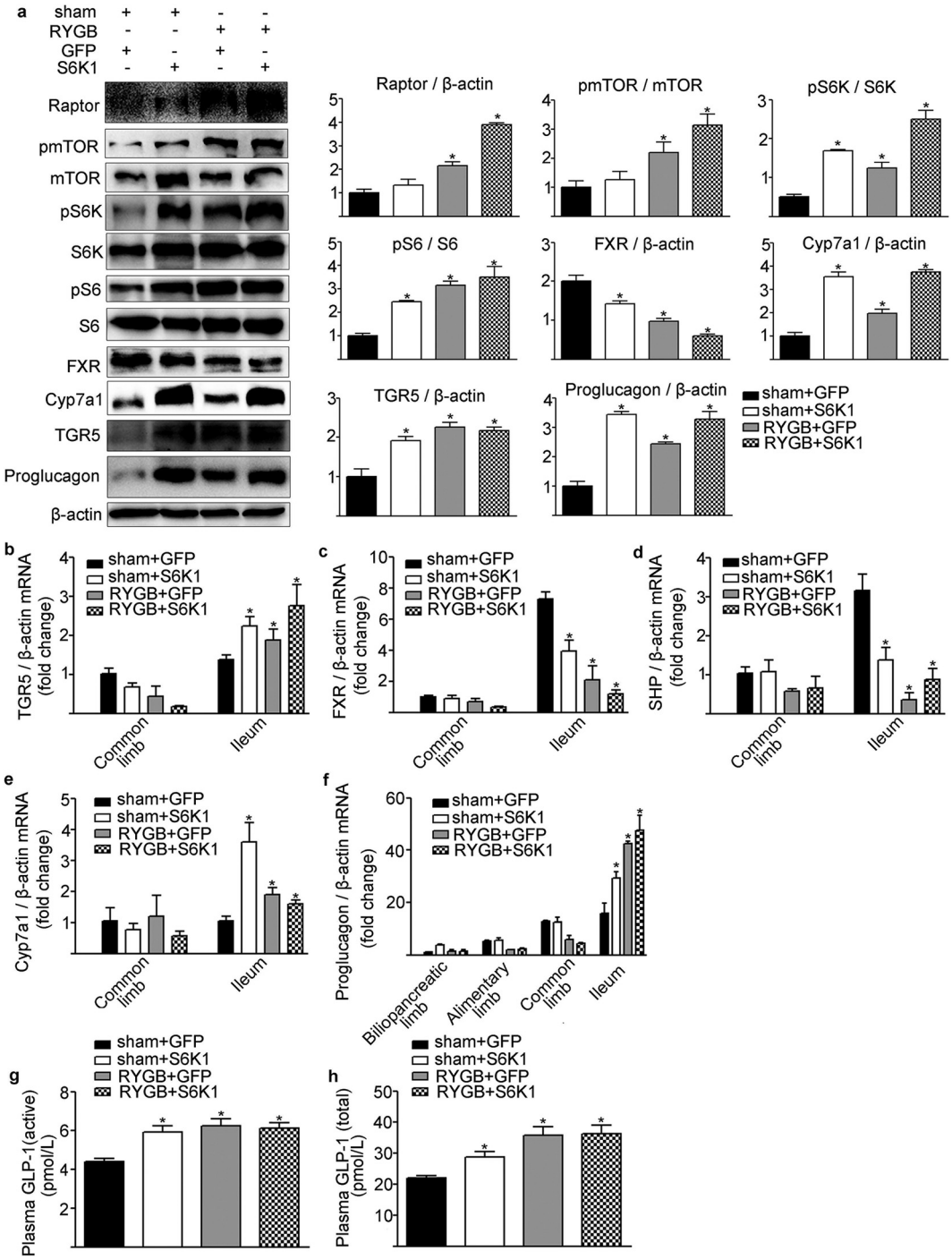

Fig. 2. Effects of Ad-S6K1 on RYGB-elicited alteration of ileal TGR5-mTORC1 signaling and GLP-1 production in DIO mice. (a) Representative western blots from sham- or RYGB- operated mice that received tail vein injection of Ad-GFP, Ad-S6K1 (10^9 pfu). Raptor, pmTOR, mTOR, pS6K, S6K, pS6, S6, FXR, Cyp7a1, TGR5, proglucagon, and β-actin were detected using specific antibodies. mRNA levels of TGR5 (b), FXR (c), SHP (d), Cyp7a1 (e) and proglucagon (f) were measured using quantitative PCR analysis. Plasma GLP-1(active) (g) and Plasma GLP-1(total) (h) were detected by ELISA. Six samples were examined for each condition. *, $P < 0.05$ vs. sham-operated mice receiving Ad-GFP. Statistical differences were assessed by factorial design ANOVA.

3.5. Stimulation of GLP-1 Synthesis and Secretion by Deoxycholic Acid in STC-1 Cells

Since RYGB significantly stimulated DCA production, the effects of DCA on GLP-1 synthesis and secretion were next examined in STC-1 cells. DCA induced a concentration- and time-dependent increase in GLP-1 synthesis and secretion (Fig. 6a–i). Further, DCA dose-dependently increased the GCG promoter activity (Fig. 6e). DCA at the doses from 3.75 to 60 μmol/L caused a concentration-dependent increase in mTORC1 activity and TGR5 levels (Fig. 6a, b).

3.6. Deoxycholic Acid Induced GLP-1 Synthesis Through TGR5-mTORC1 Signaling

Next, we examined whether mTORC1 mediates the effects of DCA on GLP-1 production. siRNA knockdown of mTOR abolished the DCA-induced increase of proglucagon mRNA and protein levels (Fig. 7a, c), as

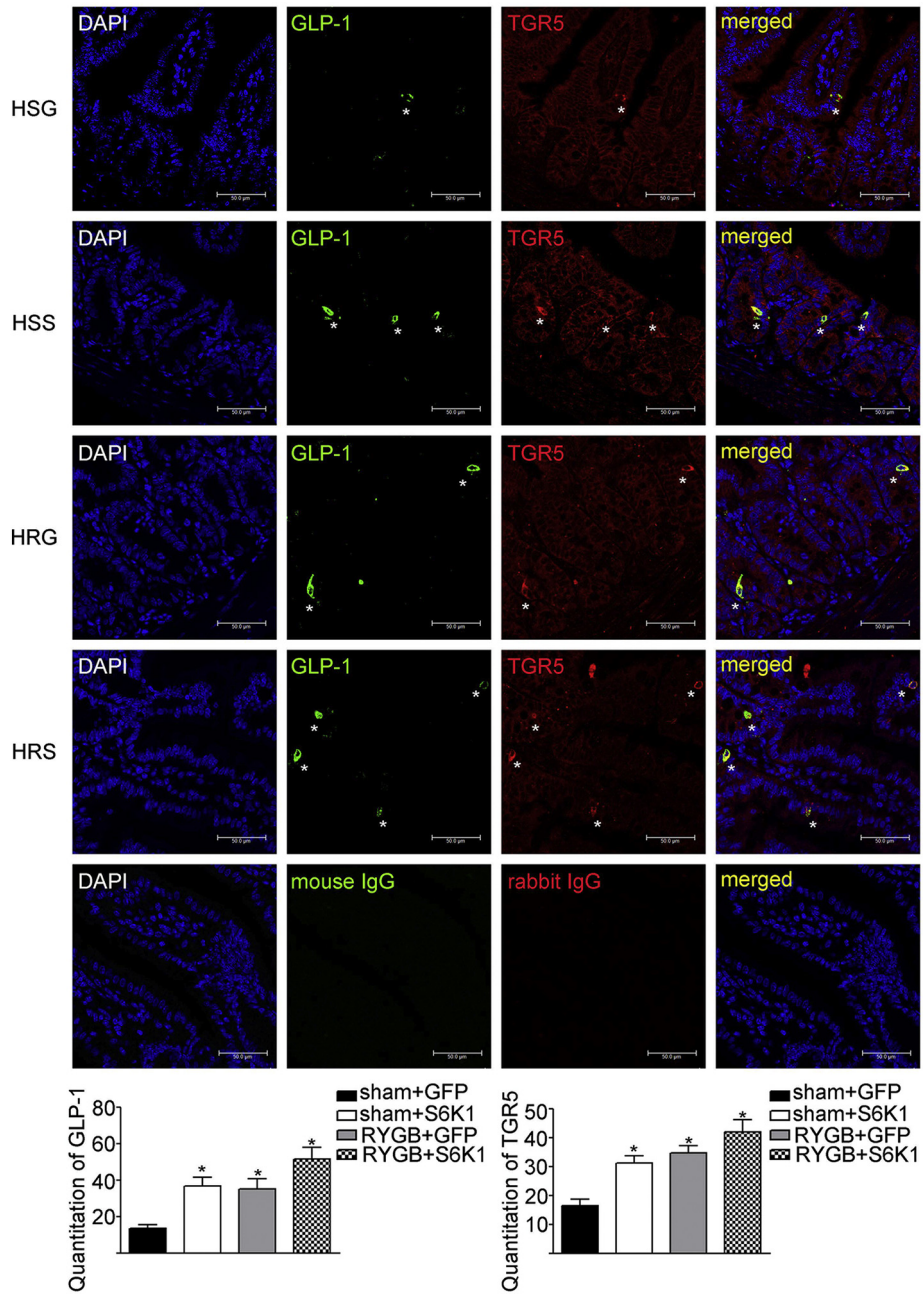

Fig. 3. Increment in co-localization of TGR5 and GLP-1 by Ad-S6K1 and RYGB. Representative images of TGR5 and GLP-1 immunostaining in ileums from sham- or RYGB- operated mice receiving Ad-GFP or Ad-S6K1. High-resolution images depicting GLP-1 (green) and TGR5 (red) in ileal mucosal cells. Merged image illustrates colocalization of GLP-1 and TGR5 (orange). Bar, 50 μm. HSG, sham-operated mice receiving Ad-GFP; HSS, sham group receiving Ad-S6K1; HRG, RYGB-operated mice receiving Ad-GFP; HRS, RYGB-operated mice receiving Ad-S6K1. Computerised image analysis (Model Leica Q550CW, Leica, Qwin, Germany) was performed to quantify the immunostaining signals of TGR5 and GLP-1 from mouse ileums. n = 6, the p value was measured with factorial design ANOVA. *, $P < 0.05$ vs. sham-operated mice receiving Ad-GFP.

well as GLP-1 secretion (Fig. 7d) in cultured STC-1 cells. Knockdown of mTOR significantly inhibited the phosphorylation of mTOR, S6K and S6, indicating a decrease in mTORC1 signaling (Fig. 7a). Furthermore, siRNA knockdown of mTOR abolished both endogenous and DCA-induced TGR5 expression (Fig. 7a, b).

TGR5 siRNA suppressed GLP-1 production induced by DCA, which was associated with inhibition of raptor expression and mTORC1 activity. Inhibition of mTORC1 activity by rapamycin also attenuated the effects of DCA on TGR5 and GLP-1 production (Fig. 7e-h).

Co-IP was further employed to investigate whether TGR5 and mTOR/raptor interacted with each other. IgGs against TGR5, raptor, and mTOR co-immunoprecipitated with each other, indicating an interaction between raptor, mTOR and TGR5. DCA treatment enhanced the interaction between TGR5 and raptor or mTOR (Fig. 7i–k).

4. Discussion

The major finding of the present study is that TGR5-mTORC1 signaling in enteric endocrine L cells contributes to the enhancement of GLP-1 production induced by RYGB. This conclusion is supported by following distinct observations: 1) A positive relationship exists among plasma bile acids, ileal mTORC1 signaling and the expression of GLP-1 during fasting; 2) RYGB stimulates ileal TGR5-mTORC1 signaling, which is associated with an increase of GLP-1 production in both lean and DIO mice;

Table 2
Plasma bile acids composition and concentrations in DIO mice receiving Ad-GFP or Ad-S6K1.

Specific BAs	HSG	HSS	HRG	HRS
3β-CA	38.8 ± 5.9	80.3 ± 14.9	133.6 ± 4.9†	93.2 ± 32.5
CA	165.7 ± 30.1	330.0 ± 207.0	549.9 ± 19.6†	3286.0 ± 1054.0‡
CDCA	35.2 ± 4.2	22.5 ± 0.4*	38.8 ± 2.5	46.1 ± 0.4§
NCA	16.7 ± 1.6	11.7 ± 2.5	14.4 ± 2.4	10.0 ± 0.1‡
UCA	8.5 ± 2.0	14.7 ± 9.9	25.3 ± 8.7	12.1 ± 1.3
α-MCA	12.7 ± 1.7	18.9 ± 1.6	66.4 ± 2.1†	25.7 ± 2.4‡
β-MCA	108.1 ± 18.4	249.7 ± 81.6	1285.0 ± 332.3†	771.8 ± 114.2‡,§
3-DHCA	17.9 ± 0.5	23.9 ± 1.0*	23.6 ± 0.3†	24.2 ± 1.7‡
7-KDCA	25.5 ± 4.0	19.5 ± 2.0	74.2 ± 0.9†	44.3 ± 5.9§
7-KLCA	42.2 ± 2.7	31.9 ± 4.8	26.1 ± 4.3†	13.7 ± 1.9‡,§
ALCA	18.1 ± 0.5	10.7 ± 0.1*	63.4 ± 1.2†	45.9 ± 10.1§
DCA	73.2 ± 19.9	133.9 ± 6.5*	481.0 ± 12.3†	426.0 ± 74.6‡,§
HDCA	33.0 ± 2.0	38.4 ± 5.2	25.4 ± 0.4†	11.3 ± 0.1‡,§
IDCA	11.2 ± 0.4	4.4 ± 0.8*	10.2 ± 1.2	23.7 ± 4.5§
UDCA	16.8 ± 2.4	43.5 ± 8.3*	94.0 ± 11.0†	100.5 ± 55.0
λ-MCA	17.3 ± 1.0	11.2 ± 5.1	15.8 ± 2.5	15.9 ± 1.0
GCA	10.3 ± 0.3	11.8 ± 4.1	15.4 ± 2.4	18.1 ± 4.5
GCDCA	13.6 ± 0.8	13.3 ± 3.5	13.4 ± 1.5	17.4 ± 1.7
TCA	301.3 ± 71.9	981.2 ± 63.7*	1794.0 ± 128.1†	2807.0 ± 215.1‡,§
α-TMCA	292.6 ± 14.9	936.3 ± 7.2*	591.8 ± 88.9†	478.5 ± 31.1‡,§
GDCA	11.4 ± 0.2	10.1 ± 0.1	14.7 ± 1.7	12.6 ± 4.1
GDHCA	7.4 ± 2.4	6.5 ± 3.1	4.4 ± 1.2	5.7 ± 0.9
GHDCA	12.5 ± 2.5	11.4 ± 3.0	9.7 ± 0.7	9.6 ± 0.1
GLCA	8.8 ± 1.5	14.1 ± 1.1*	12.7 ± 2.7	20.2 ± 4.4
GUDCA	16.5 ± 2.8	15.2 ± 2.3	14.7 ± 1.0	10.3 ± 0.4
TDCA	59.8 ± 3.3	58.2 ± 5.8	111.1 ± 0.1†	72.8 ± 3.2‡
THDCA	19.6 ± 3.1	24.2 ± 5.6	10.4 ± 0.5†	8.3 ± 0.8‡,§
TLCA	8.5 ± 0.3	10.2 ± 1.6	11.3 ± 2.3	6.7 ± 0.7
TUDCA	35.1 ± 1.6	99.7 ± 14.2*	140.6 ± 12.7†	155.5 ± 33.2‡
λ-GMCA	16.9 ± 1.6	11.7 ± 3.4	13.7 ± 0.8	11.0 ± 2.9
λ-TMCA	134.6 ± 16.7	1408.0 ± 166.7*	2122.0 ± 333.3†	2345.0 ± 333.3‡
Total BAs	1592.0 ± 40.1	4655.0 ± 201.7*	7810.0 ± 919.3†	10,900.0 ± 951.0‡,§
Unconjugated BAs	647.8 ± 38.1	1043.0 ± 306.4 *	2931.0 ± 365.6†	4926.0 ± 852.8‡,§
Conjugated BAs	949.0 ± 58.6	3612.0 ± 105.1*	4879.0 ± 554.1†	5978.0 ± 98.6‡,§
Primary BAs	1004.0 ± 49.2	2670.0 ± 359.0*	4527.0 ± 556.2†	7566.0 ± 767.0‡,§
Secondary BAs	588.0 ± 31.2	1985.0 ± 158.2*	3283.0 ± 363.3†	3338.0 ± 199.1‡,§

Values are presented as the mean ± SEM. All bile acids are presented in concentrations of nmol/L (n = 5 per group).
* $P < 0.05$ within sham-operated mice receiving Ad-GFP (HSG) vs sham group receiving Ad-S6K1 (HSS).
† $P < 0.05$ within HSG vs RYGB-operated mice receiving Ad-GFP (HRG).
‡ $P < 0.05$ within HSG vs RYGB-operated mice receiving Ad-S6K1 (HRS).
§ $P < 0.05$ within HSS vs HRS.

3) Rapamycin attenuates the effect of RYGB on TGR5-mTORC1 signaling and GLP-1 production; 4) Both RYGB and overexpression of S6K1 enhance the TGR5-mTORC1 signaling, leading to subsequent increase in GLP-1 production; 5) Ileal TGR5-mTORC1 signaling and GLP-1 production are significantly increased in post-RYGB patients compared to obese type 2 diabetic patients; 6) RYGB-induced increase of GLP-1 production correlates with plasma bile acids, particularly DCA; 7) DCA stimulates TGR5-mTORC1 signaling and GLP-1 production in STC-1 cells; 8) Both TGR5 siRNA and mTOR siRNA abolish the stimulation of GLP-1 production induced by DCA; 9) DCA increases the interaction between TGR5 and mTOR/Raptor.

RYGB, the most commonly performed bariatric operation, ameliorates virtually all obesity-related comorbid conditions, the most impressive being a dramatic resolution of type 2 diabetes mellitus (T2DM). After RYGB, 84% of patients with T2DM experience complete remission of this disease, and virtually all have improved glycemic control [39]. Several mechanisms probably mediate the antidiabetic impact of RYGB, including enhanced GLP-1 release from L cells [5,6,10,39]. Numerous animal and human studies that have examined changes in the release of GLP-1 after RYGB have consistently illustrated that fasting levels of GLP-1 are increased by several folds [6,10,39]. The mechanism underlying the up-regulation of GLP-1 after RYGB remains largely unknown. Rapid delivery of food to the incretin-secreting portions of the intestine has been presumed to account for the increase in GLP-1 after meal ingestion in post-RYGB patients [40]. An increase in L-cell number has also been attributed to the enhanced proglucagon expression induced by RYGB in rats [41]. Our studies demonstrate that ileal mTORC1 signaling contributes to the increase of GLP-1 production after RYGB. mTORC1 signaling activity in ileal mucosa is up-regulated after RYGB in both rodents and human subjects. Suppression of mTORC1 activity attenuates the effects of RYGB on GLP-1 production. These findings are consistent with our previous study showing that mTORC1 signaling in intestinal mucosa coordinates overall fuel levels with production and secretion of GLP-1 [30].

As the biomarkers for diabetes and obesity, plasma levels of bile acids are positively related to glycemic control [42]. Lowering circulating bile acids worsens diet-induced obesity and diabetes, whereas increasing bile acid pool size improves glucose homeostasis [19]. Recent studies also suggest a mechanistic role for bile acids in the metabolic improvement following bariatric surgery. Fasting BAs increase after RYGB [19]. By activating FXR and TGR5, bile acids facilitate postprandial absorption of nutrients and regulate lipid, glucose and energy metabolism [19,42]. In enteroendocrine L cells, bile acids regulate the synthesis and secretion of GLP-1 via its counteracting effects on transmembrane receptor TGR5 and nuclear receptor FXR [19,22,23,37]. Deletion of TGR5 completely abolishes the up-regulation of ileal proglucagon and plasma GLP-1 following VSG surgery [20,21]. In our study, we found that after RYGB, concentrations of most circulating unconjugated and conjugated BAs were significantly increased and TGR5 signaling in ileums were activated in rodents. Both western blot and immunofluorescent staining demonstrate significantly higher levels of TGR5 in L cells after RYGB surgery. The potency order of BAs to activate TGR5 and FXR is: LCA > DCA > CDCA>CA and CDCA>DCA > CA > LCA respectively [19]. The observation that DCA, an agonist for both TGR5 and FXR, is significantly increased

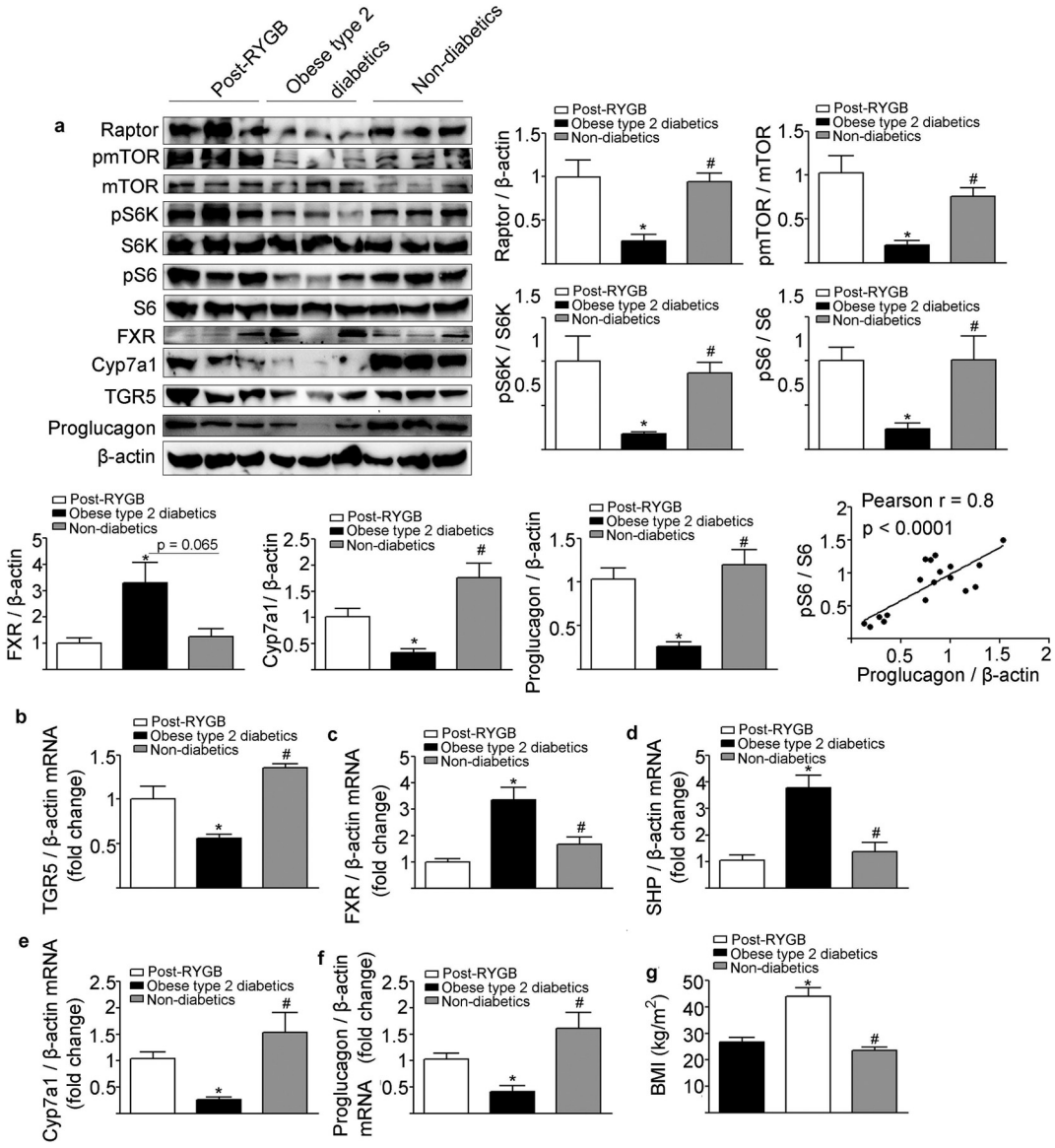

Fig. 4. Effects of RYGB on ileal TGR5-mTORC1 signaling and GLP-1 production in human beings. (a) Representative western blot from ileums of non-diabetic subjects, obese type 2 diabetics, post-RYGB patients. Raptor, pmTOR, mTOR, pS6K, S6K, pS6, S6, FXR, Cyp7a1, TGR5, and proglucagon were blotted. mTOR, S6K, S6, and β-actin were used as loading controls. Quantification of image analysis of intestinal S6 phosphorylation and proglucagon expression is expressed as mean ± SEM. Correlations between protein levels of proglucagon/β-actin and pS6/S6 were determined by Pearson analysis. Results of quantitative PCR analysis of TGR5 mRNA (b), FXR mRNA (c), SHP mRNA (d), Cyp7a1 mRNA (e) and proglucagon mRNA (f) are expressed as fold change from lean post-RYGB subjects using β-actin as loading control. (g) Body mass index (BMI) for human subjects. n = 6, *, $P < 0.05$ vs. Post-RYGB subjects. #, $P < 0.05$ vs. obese type 2 diabetics. Statistical differences were assessed by one-way ANOVA followed by Newman-Student-Keuls test.

informs us to examine whether DCA-TGR5/FXR signaling is enhanced in L cells after RYGB. Although mice have markedly different bile acid profile than humans, it has been reported that serum DCA increases significantly after RYGB in both rodent and human subjects [43,44]. DCA may thus function as a major BA to stimulate the synthesis of GLP-1 after RYGB. The increase in ileal TGR5 signaling subsequently recruits mTOR complex 1 to alter GLP-1 production. Our in vitro data further support this hypothesis. Treatment of STC-1 cells with DCA activates mTORC1 signaling, which is subsequently followed with the increase of GLP-1 production. Suppression of mTORC1 signaling by rapamycin or silence of mTOR gene attenuates the effect of DCA. TGR5 deficiency significantly reduces the effect of DCA on mTORC1 signaling and subsequent GLP-1 production. Consistent with our observation, previous study also demonstrates that activation of TGR5 stimulates mTORC1 signaling in macrophage [45]. Limitations exist for our approaches that seek to assess the link between TGR5 and mTORC1 in vivo. Chronic treatment of mice with a TGR5 agonist will address this potential. Since TGR5 antibodies lack specificity, additional studies using TGR5 gene null mice should be performed to confirm the specificity of the applied antibody. Further, since DCA constitutes only <15% of total circulating BAs, it is worth of noting that signaling pathway in addition to mTORC1 may mediate the effects of increased BAs on the upregulation of GLP-1 after RYGB surgery. Limitations also exist in our human study. RYGB was only compared to obese diabetics but not to obese non-diabetics. Further studies on obese non-diabetic patients will address this potential.

Alteration in bile acid composition also activates FXR, whose activity has been reported to repress proglucagon gene expression and GLP-1 secretion in the ileum [37]. In our study, ileal FXR expression is significantly lower after RYGB. Since FXR inhibits mTOR-S6K signaling pathway in liver cancer cells [46], reduction of ileal FXR may contribute to the hyperactivation of mTORC1 signaling after RYGB operation.

In summary, our studies demonstrate that RYGB increases deoxycholic acid-TGR5 signaling, which subsequently activates mTORC1

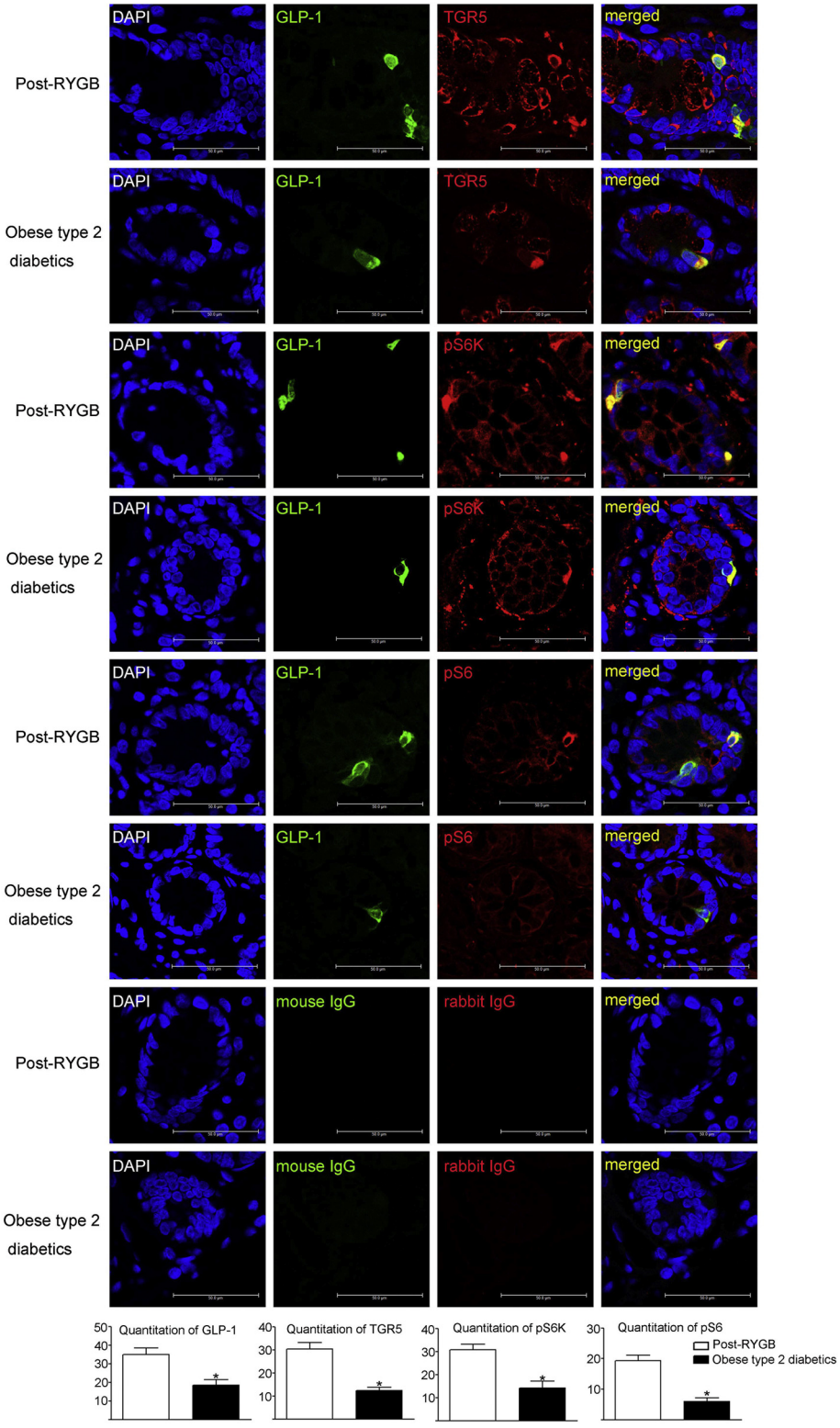

Fig. 5. Immunofluorescent analysis of TGR5 and GLP-1 in the human ileal mucosa in obese and post-RYGB subjects. Expression and colocalization of TGR5 (red), pS6K(red) or pS6 (red) and GLP-1 (green) in the human ileal mucosa in obese type 2 diabetic patients and post-RYGB subjects. Merged image (orange) illustrates colocalization of TGR5, pS6K or pS6 and GLP-1. Bar, 50 μm. Computerised image analysis (Model Leica Q550CW, Leica, Qwin, Germany) was performed to quantify the immunostaining signals of TGR5, GLP-1, pS6K, and pS6 from human ileal mucosa. The p value was measured with Student's t-test. n = 5, *, $P < 0.05$ vs. post-RYGB subjects.

signaling to stimulate GLP-1 production in L cells (Fig. 8). TGR5-mTORC1 signaling may represent a novel mechanism responsible for the metabolic benefit of RYGB, thus providing a potential target for the intervention of obesity and diabetes.

Acknowledgments

We thank Guosheng Liang from University of Texas Southwestern Medical Center for critical reading of the manuscript.

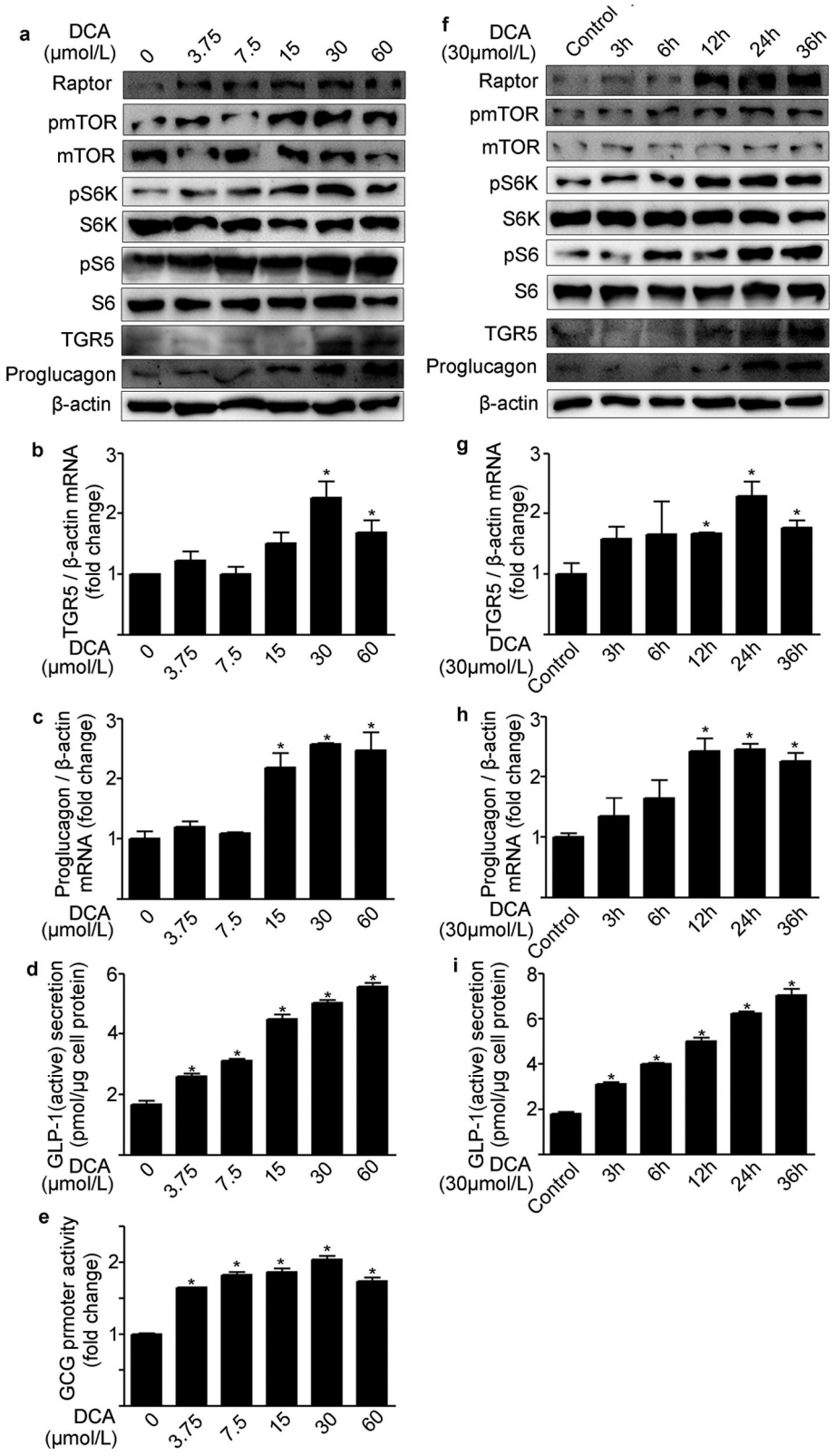

Fig. 6. Stimulation of GLP-1 synthesis and secretion by DCA in STC-1 cells. Cultured STC-1 cells were treated with various concentrations of DCA for 24 h (a-e), or DCA (30 μmol/L) for time indicated (f-i). TGR5 mRNA (b, g), proglucagon mRNA (c, h) and protein (a, f) were analyzed by RT-PCR and western blotting. Medium GLP-1 (d, i) was determined by enzyme immunoassay. (e) Proglucagon promoter activity, Luciferase activity with the dual-luciferase reporter assay system was measured using a luminometer. Results are expressed as mean ± SEM. Experiments were repeated for three times. The p value was measured with Student's t-test. *, $P < 0.05$ vs. control.

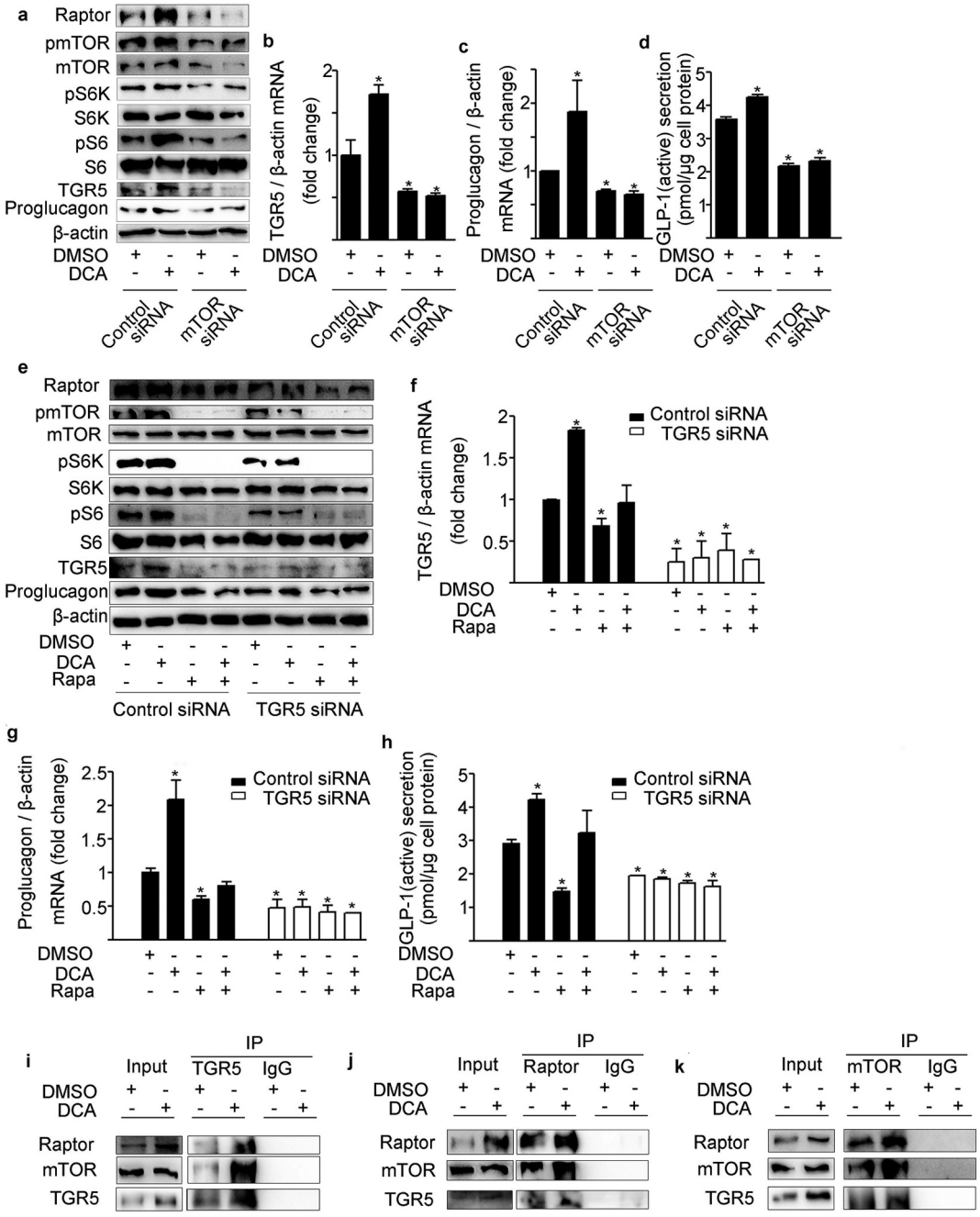

Fig. 7. Modulation of GLP-1 production by DCA through TGR5-mTORC1 signaling. STC-1 cells were transfected with control siRNA or mTOR siRNA and treated with DMSO or DCA (30 μmol/L) for 24 h. Results were expressed as mean ± SEM. n = 3. *, $P < 0.05$ vs. control. (a) Representative western blots of Raptor, pmTOR, mTOR, pS6K, S6K, pS6, S6, TGR5, proglucagon and β-actin. (b) TGR5 mRNA. (c) Proglucagon mRNA. (d) Medium GLP-1(active) concentration. STC-1 cells were transfected with control siRNA or TGR5 siRNA and treated with following drugs for 24 h: DMSO, DCA (30 μmol/L), rapamycin (50 nmol/L) or DCA plus rapamycin. Results were expressed as mean ± SEM. n = 3. *, $P < 0.05$ vs. control. (e) Representative western blots of Raptor, pmTOR, mTOR, pS6K, S6K, pS6, S6, TGR5, proglucagon and β-actin. (f) TGR5 mRNA. (g) Proglucagon mRNA. (h) Medium GLP-1(active) concentration. (i-k) Immunoprecipitations/Immunoblot assaying for interaction between endogenous TGR5 and Raptor/mTOR. STC-1 cells were treated with DMSO or DCA (30 μmol/L) for 24 h. The interaction between TGR5 and Raptor/mTOR was detected by co-immunoprecipitation. TGR5 was precipitated using anti-TGR5 antibodies and co-precipitated mTOR and Raptor were immunoblotted (i). Raptor was precipitated using anti-Raptor antibodies and co-precipitated mTOR and TGR5 were immunoblotted under DMSO or DCA treatment (j). mTOR was precipitated using anti-mTOR antibodies and co-precipitated Raptor and TGR5 were immunoblotted under DMSO or DCA treatment (k).

Funding

This work was supported by grants from the National Natural Science Foundation of China (81770794, 31401001, 81730020), the Science and Technology Planning Project of Guangdong Province, China (2014A020212210), the Natural Science Foundation of Guangdong Province (2016A030310086), the Special Grants from the Guangzhou Pearl River Young Talents of Science and Technology (201610010079), the Guangzhou Science and Technology Project (2014Y2-00097), the Fundamental Research Funds for the Central Universities (21617457).

Conflicts of Interest

There are no conflicts of interest.

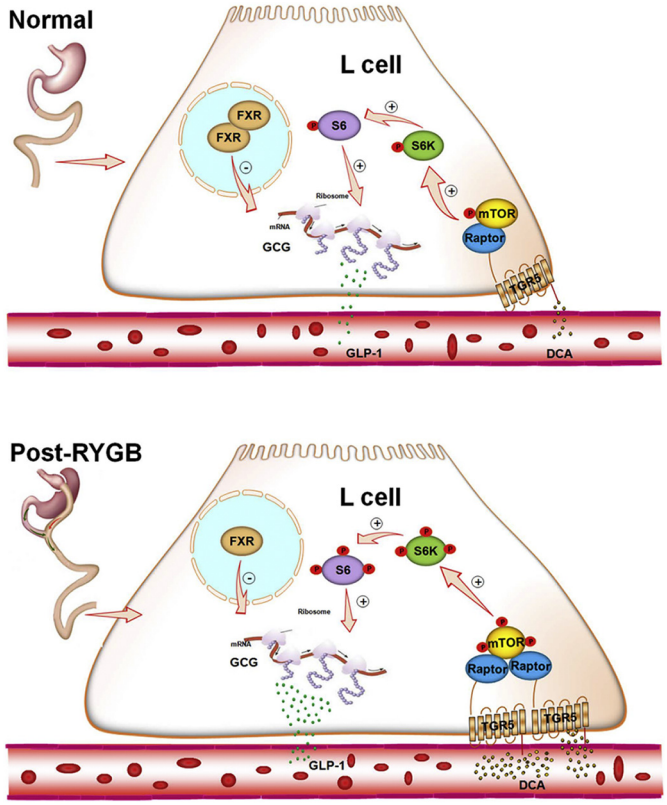

Fig. 8. Summary of putative mechanisms linking TGR5-mTORC1 signaling pathway and GLP-1 production after Roux-en-Y gastric bypass. After RYGB, circulating bile acids and ileal TGR5 are elevated, whereas FXR is down-regulated. This concurrent increase of TGR5 and decrease of FXR stimulates mTORC1 signaling, leading to the subsequent stimulation of GLP-1 production.

Author Contributions

G.X. and W.Z. designed the study. H.Z., Z.L., M.P., Z.H., T.Q., L.C., H.L. and H.Z. performed the experiments. H.Z., Z.L., M.P. and G.X. analyzed the data. G.X. and W.Z. drafted the manuscript. H.Z., Z.L., M.P., G.X. and W.Z. contributed to the interpretation of the results and critical revision of the manuscript for important intellectual content and approved the final version of the manuscript. H.Z., G.X. and W.Z. obtained funding. G.X. is the guarantor of this work and, as such, had full access to all the data in the study and takes responsibility for the integrity of the data and the accuracy of the data analysis.

Ethical Approval

The biopsy specimens were obtained under protocols approved by the Research Ethics Committee of the First Affiliated Hospital of Jinan University. Informed consent was obtained from all patients. All animal experiments were undertaken with approval from the Laboratory Animal Ethics Committee of Jinan University.

Appendix A. Supplementary Data

Supplementary data to this article can be found online at https://doi.org/10.1016/j.ebiom.2018.05.026.

References

[1] Nguyen NT, Nguyen XM, Lane J, Wang P. Relationship between obesity and diabetes in a US adult population: findings from the National Health and Nutrition Examination Survey, 1999–2006. Obes Surg 2011;21:351–5.
[2] Kushner RF. Weight loss strategies for treatment of obesity. Prog Cardiovasc Dis 2014;56:465–72.
[3] Mingrone G, Panunzi S, De Gaetano A, et al. Bariatric surgery versus conventional medical therapy for type 2 diabetes. N Engl J Med 2012;366:1577–85.
[4] Cummings DE, Weigle DS, Frayo RS, et al. Plasma ghrelin levels after diet-induced weight loss or gastric bypass surgery. N Engl J Med 2002;346:1623–30.
[5] Kellum JM, Kuemmerle JF, O'Dorisio TM, et al. Gastrointestinal hormone responses to meals before and after gastric bypass and vertical banded gastroplasty. Ann Surg 1990;211:763–70.
[6] le Roux CW, Aylwin SJ, Batterham RL, et al. Gut hormone profiles following bariatric surgery favor an anorectic state, facilitate weight loss, and improve metabolic parameters. Ann Surg 2006;243:108–14.
[7] Rodieux F, Giusti V, D'Alessio DA, Suter M, Tappy L. Effects of gastric bypass and gastric banding on glucose kinetics and gut hormone release. Obesity (Silver Spring) 2008;16:298–305.
[8] Hutch CR, Sandoval D. The role of GLP-1 in the metabolic success bariatric surgery. Endocrinology 2017;158:4139–51.
[9] Laferrère B, Teixeira J, McGinty J, et al. Effect of weight loss by gastric bypass surgery versus hypocaloric diet on glucose and incretin levels in patients with type 2 diabetes. J Clin Endocrinol Metab 2008;93:2479–85.
[10] Shah M, Law JH, Micheletto F, et al. Contribution of endogenous glucagon-like peptide 1 to glucose metabolism after Roux-en-Y gastric bypass. Diabetes 2014;63:483–93.
[11] Baggio LL, Drucker DJ. Biology of incretins: GLP-1 and GIP. Gastroenterology 2007;132:2131–57.
[12] Ayala JE, Bracy DP, James FD, Julien BM, Wasserman DH, Drucker DJ. The glucagon-like peptide-1 receptor regulates endogenous glucose production and muscle glucose uptake independent of its incretin action. Endocrinology 2009;150:1155–64.
[13] Flint A, Raben A, Ersbøll AK, Holst JJ, Astrup A. The effect of physiological levels of glucagon-like peptide-1 on appetite, gastric emptying, energy and substrate metabolism in obesity. Int J Obes Relat Metab Disord 2001;25:781–92.
[14] Deacon CF, Johnsen AH, Holst JJ. Degradation of glucagon-like peptide-1 by human plasma in vitro yields an N-terminally truncated peptide that is a major endogenous metabolite in vivo. J Clin Endocrinol Metab 1995;80:952–7.
[15] Vahl TP, Paty BW, Fuller BD, Prigeon RL, D'Alessio DA. Effects of GLP-1-(7-36)NH2, GLP-1-(7-37), and GLP-1- (9-36)NH2 on intravenous glucose tolerance and glucose-induced insulin secretion in healthy humans. J Clin Endocrinol Metab 2003;88:1772–9.
[16] Drucker DJ, Nauck MA. The incretin system: glucagon-like peptide-1 receptor agonists and dipeptidyl peptidase-4 inhibitors in type 2 diabetes. Lancet 2006;368:1696–705.
[17] Meier JJ. GLP-1 receptor agonists for individualized treatment of type 2 diabetes mellitus. Nat Rev Endocrinol 2012;8:728–42.
[18] Kaska L, Sledzinski T, Chomiczewska A, Dettlaff-Pokora A, Swierczynski J. Improved glucose metabolism following bariatric surgery is associated with increased circulating bile acid concentrations and remodeling of the gut microbiome. World J Gastroenterol 2016;22:8698–719.
[19] Chávez-Talavera O, Tailleux A, Lefebvre P, Staels B. Bile acid control of metabolism and inflammation in obesity, type 2 diabetes, dyslipidemia, and nonalcoholic fatty liver disease. Gastroenterology 2017;152:1679–94.
[20] Ding L, Sousa KM, Jin L, et al. Vertical sleeve gastrectomy activates GPBAR-1/TGR5 to sustain weight loss, improve fatty liver, and remit insulin resistance in mice. Hepatology 2016;64:760–73.
[21] McGavigan AK, Garibay D, Henseler ZM, et al. TGR5 contributes to glucoregulatory improvements after vertical sleeve gastrectomy in mice. Gut 2017;66:226–34.
[22] Brighton CA, Rievaj J, Kuhre RE, et al. Bile acids trigger GLP-1 release predominantly by accessing basolaterally located G protein-coupled bile acid receptors. Endocrinology 2015;156:3961–70.
[23] Thomas C, Gioiello A, Noriega L, et al. TGR5-mediated bile acid sensing controls glucose homeostasis. Cell Metab 2009;10:167–77.
[24] Dennis PB, Jaeschke A, Saitoh M, Fowler B, Kozma SC, Thomas G. Mammalian TOR: a homeostatic ATP sensor. Science 2001;294:1102–5.
[25] Yang Q, Guan KL. Expanding mTOR signaling. Cell Res 2007;17:666–81.
[26] Laplante M, Sabatini DM. mTOR signaling in growth control and disease. Cell 2012;149:274–93.
[27] Saxton RA, Sabatini DM. mTOR signaling in growth metabolism, and disease. Cell 2017;168:960–76.
[28] Le Bacquer O, Petroulakis E, Paglialunga S, et al. Elevated sensitivity to diet-induced obesity and insulin resistance in mice lacking 4E-BP1 and 4E-BP2. J Clin Invest 2007;117:387–96.
[29] Um SH, Frigerio F, Watanabe M, et al. Absence of S6K1 protects against age- and diet-induced obesity while enhancing insulin sensitivity. Nature 2004;431:200–5.
[30] Xu G, Li Z, Ding L, et al. Intestinal mTOR regulates GLP-1 production in mouse L cells. Diabetologia 2015;58:1887–97.
[31] Bruinsma BG, Uygun K, Yarmush ML, Saeidi N. Surgical models of Roux-en-Y gastric bypass surgery and sleeve gastrectomy in rats and mice. Nat Protoc 2015;10:495–507.
[32] Hao Z, Zhao Z, Berthoud HR, Ye J. Development and verification of a mouse model for Roux-en-Y gastric bypass surgery with a small gastric pouch. PLoS One 2013;8:e52922.
[33] Uchida A, Zechner JF, Mani BK, Park WM, Aguirre V, Zigman JM. Altered ghrelin secretion in mice in response to diet-induced obesity and Roux-en-Y gastric bypass. Mol Metab 2014;3:717–30.
[34] Xu G, Hong X, Tang H, et al. Ghrelin regulates GLP-1 production through mTOR signaling in L cells. Mol Cell Endocrinol 2015;416:9–18.
[35] Anderwald CH, Tura A, Promintzer-Schifferl M, et al. Alterations in gastrointestinal, endocrine, and metabolic processes after bariatric Roux-en-Y gastric bypass surgery. Diabetes Care 2012;35:2580–7.

[36] Myant NB, Mitropoulos KA. Cholesterol 7 alpha-hydroxylase. J Lipid Res 1977;18:135–53.
[37] Trabelsi MS, Daoudi M, Prawitt J, et al. Farnesoid X receptor inhibits glucagon-like peptide-1production by enteroendocrine L cells. Nat Commun 2015;6:7629.
[38] Katsuma S, Hirasawa A, Tsujimoto G. Bile acids promote glucagon-like peptide-1 secretion through TGR5 in a murine enteroendocrine cell line STC-1. Biochem Biophys Res Commun 2005;329:386–90.
[39] Cummings DE. Endocrine mechanisms mediating remission of diabetes after gastric bypass surgery. Int J Obes (Lond) 2009;33(Suppl. 1):S33–40.
[40] Ten Kulve JS, Veltman DJ, Gerdes VEA, et al. Elevated postoperative endogenous GLP-1 levels mediate effects of Roux-en-Y gastric bypass on neural responsivity to food cues. Diabetes Care 2017;40:1522–9.
[41] Hansen CF, Bueter M, Theis N, et al. Hypertrophy dependent doubling of L-cells in Roux-en-Y gastric bypass operated rats. PLoS One 2013;8:e65696.
[42] Li T, Francl JM, Boehme S, et al. Glucose and insulin induction of bile acid synthesis mechanisms and implication in diabetes and obesity. J Biol Chem 2012;287:1861–73.
[43] Simonen M, Dali-Youcef N, Kaminska D, et al. Conjugated bile acids associate with altered rates of glucose and lipid oxidation after Roux-en-Y gastric bypass. Obes Surg 2012;22:1473–80.
[44] Spinelli V, Lalloyer F, Baud G, et al. Influence of Roux-en-Y gastric bypass on plasma bile acid profiles: a comparative study between rats, pigs and humans. Int J Obes (Lond) 2016;40:1260–7.
[45] Perino A, Pols TW, Nomura M, Stein S, Pellicciari R, Schoonjans K. TGR5 reduces macrophage migration through mTOR-induced C/EBPβ differential translation. J Clin Invest 2014;124:5424–36.
[46] Huang X, Zeng Y, Wang X, et al. FXR blocks the growth of liver cancer cells through inhibiting mTOR-s6K pathway. Biochem Biophys Res Commun 2016;474:351–6.